Available online at www.sciencedirect.com
ScienceDirect
Signal Processing 87 (2007) 1597–1612
SIGNAL PROCESSING
www.elsevier.com/locate/sigpro

Perturbation analysis of conjugate MI-ESPRIT for single acoustic vector-sensor-based noncircular signal direction finding ☆

Yougen Xu*, Zhiwen Liu, Jinliang Cao

Department of Electronic Engineering, Beijing Institute of Technology, Beijing 100081, People's Republic of China

Received 21 July 2006; received in revised form 31 October 2006; accepted 27 December 2006
Available online 16 January 2007

Abstract

The closed-form conjugate multiple-invariance ESPRIT (CMI-ESPRIT) algorithm herein analyzed: (1) makes use of redundancy in the nonvanishing conjugated second- and fourth-order cumulants of noncircular signals; (2) recognizes the real-valued two-dimensional directivity inherently achieved by an acoustic vector-sensor in a free-space. It is provided in this correspondence the perturbation analyses on both the norm-penalized and the subspace-constraint ESPRIT matrices that play the key role in the CMI-ESPRIT. It is shown that the norm-penalized ESPRIT matrix is biased (but bounded) and has a minimal mean-squared-error (MSE) for some finite regularization factor, whereas the subspace-constraint ESPRIT matrix is unbiased and its MSE approaches minimum when the regularization factor becomes infinite. These observations are potentially useful for the determination of the regularization parameters which is significant for the performance of CMI-ESPRIT. The results also contribute to the ultimate study of direction-finding accuracy. Simulation results are presented to validate the given analyses.

Keywords: Antenna arrays; Array signal processing; Direction-of-arrival estimation; Acoustic array

1. Introduction

Acoustic vector-sensors have attracted increasing interest for direction-finding and beamforming [1–3]. A "complete" acoustic vector-sensor such as a vector-hydrophone consists of a pressure sensor and a collocated triad of three orthogonal velocity sensors [1]. These four sensors together measure the scalar acoustic pressure and all three components of the acoustic particle velocity vector of the incident acoustic wave-field at a given point. In contrast, an "incomplete" acoustic vector-sensor only consists of a subset of the above four-component sensors, for example, a three-component vector hydrophone formed from any two

☆This work was supported by the Specialized Research Fund for the Doctoral Program of Higher Education under Grant No. 20040007013.
*Corresponding author.
E-mail address: yougenxu@bit.edu.cn (Y. Xu).

0165-1684/$ - see front matter © 2007 Elsevier B.V. All rights reserved.
doi:10.1016/j.sigpro.2006.12.016

orthogonally oriented velocity-hydrophones plus a pressure-hydrophone [4]. Currently, a variety of subspace-based direction-finding algorithms have been developed for acoustic vector-sensors [4–9].

Very recently, noncircularity-exploitation in array signal processing mainly for aperture extension is advocated by some researchers. For instance, a new root-finding scheme taking noncircularity into account for direction-of-arrival (DOA) estimation was proposed in [10], wherein the number of sources that can be handled may exceed the number of sensors in the array. Moreover, it was shown in [11] that noncircularity of source could be utilized to significantly improve the accuracy of unitary-ESPRIT-based direction-finding in the modern communications systems. Noncircularity has also been used in blind source separation [12]. Some other work on performance evaluation of noncircular signal direction finding can be found in [13,14].

In the context of direction-finding with only one acoustic vector-sensor in a free space, temporal structure of signal has been exploited for development of *closed-form* direction-finding algorithms such as the temporal *estimation of signal parameters* via *rotational invariance techniques* (ESPRIT) [15], which was suggested in [4]. Differently from the original spatial ESPRIT [15], this interesting method does not require that a number of matched sensor-pairs are present in the array. However, it is necessary that the signals of interest have distinct carrier frequencies. In this paper, we consider the problem of noncircular signal direction-finding with an acoustic vector-sensor. In such a case we have multiple rotational invariances to be exploited for improving the estimation performance. Multiple invariance ESPRIT (MI-ESPRIT [19]), via *nonlinear* least-squares fitting (LSF) (also known as subspace fitting), represents a good candidate for this purpose. However, involving a nonlinear and iterative optimization, MI-ESPRIT sacrifices the computation advantage of the standard ESPRIT using only one invariance [15]. In contrast, the efficient full-aperture conjugate MI-ESPRIT algorithm described here (see also [16]) requires only *linear* LSF. The main aim of this paper is to give a perturbation analysis on the so-called ESPRIT matrix which greatly influences the behavior of conjugate MI-ESPRIT. The obtained results may serve as the foundation of the final examination of DOA estimation accuracy.

This paper is organized as follows. In Section 2, we introduce the model assumptions, necessary notations, and data statistics. We then describe in Section 3 the conjugate MI-ESPRIT. The perturbation analyses for two types of ESPRIT matrices calculated in the conjugate MI-ESPRIT are respectively provided in Section 4 and Section 5. We then present some simulation results in Section 6 to support our analyses. Finally, we conclude the paper in Section 7.

2. Model assumptions, notations, and data statistics

2.1. Vector-sensor measurements

It is assumed that the acoustic wave is traveling in a quiescent, homogeneous, and isotropic fluid, and is from a source of azimuth θ and elevation ϕ, where $0 \leqslant \theta \leqslant 2\pi$ and $0 \leqslant \phi \leqslant \pi$ are, respectively, measured from the positive x-axis and the positive z-axis (see Fig. 1). Then, the "complete" acoustic vector-sensor's 4×1 array

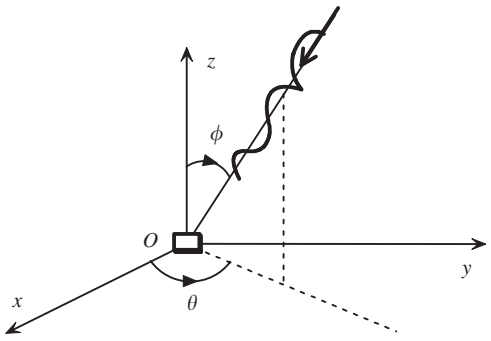

Fig. 1. Coordinate system and angle definition.

response vector in a free space can be modeled as [1]

$$\mathbf{a}(\theta,\phi)=\begin{pmatrix}\cos(\theta)\sin(\phi)\\ \sin(\theta)\sin(\phi)\\ \cos(\phi)\\ 1\end{pmatrix}=\begin{pmatrix}u_x\\ u_y\\ u_z\\ 1\end{pmatrix}, \tag{1}$$

where u_x, u_y, and u_z are three direction-cosines along the x-, y-, and z-axis, respectively. This two-dimensional azimuth-elevation directivity is *real-valued* and independent of signal carrier-frequency and hence signal bandwidth.

2.2. Noncircular signal model

Assume that Q acoustic signals impinge upon the acoustic vector-sensor, then the univector-sensor output is given by

$$\mathbf{r}(t)=\sum_{p=1}^{Q}\mathbf{a}_p s_p(t)+\mathbf{n}(t)=\mathbf{A}\mathbf{s}(t)+\mathbf{n}(t) \tag{2}$$

where $\mathbf{a}_p \overset{\text{def}}{=} \mathbf{a}(\theta_p,\phi_p)$, $\mathbf{A}\overset{\text{def}}{=}[\mathbf{a}_1,\ldots,\mathbf{a}_Q]$, $\mathbf{s}(t)\overset{\text{def}}{=}[s_1(t),\ldots,s_Q(t)]^{\mathrm{T}}$ is the signal vector, and $\mathbf{n}(t)$ is the additive noise term. It is assumed that $\mathbf{n}(t)$ is white Gaussian noise of zero-mean, and, for any lag τ,

$$\begin{cases} E(\mathbf{n}(t)\mathbf{n}^{\mathrm{T}}(t+\tau))=\mathbf{O}_{4,4},\\ E(\mathbf{n}(t)\mathbf{n}^{\mathrm{H}}(t+\tau))=\sigma_n^2\delta(\tau)\mathbf{I}_4,\\ E(\mathbf{n}(t)s_p(t+\tau))=\mathbf{0}_4,\ \ p=1,2,\ldots,Q,\end{cases} \tag{3}$$

where "T" and "H" denote transpose and conjugate transpose, respectively, "E" denotes statistical expectation, $\delta(t)$ denotes the Kronecker delta, $\mathbf{I}_G$ and $\mathbf{O}_{G,G'}$ represent the $G\times G$ identity matrix and $G\times G'$ zero matrix, respectively, $\mathbf{0}_G$ denotes the $G\times 1$ zero vector. We next will suppress the dimension index when this does not cause any confusion.

A signal $s(t)$ is said to be noncircular if $E(s^2(t))\neq 0$, and we here assume $E(s_p^2(t))\neq 0$ for $p=1,2,\ldots,Q$. Particularly, for signals that have linear constellation such as a *binary phase shift keying* (BPSK) signal (of form $s_p(t)=e^{j\varphi_p}m_p(t)$, where $m_p(t)=m_p^*(t)$) which may find applications in the underwater communications systems (see [20–22], and references therein), we have the following observation vector:

$$\mathbf{x}(t)=\mathbf{A}\mathbf{\Phi}\mathbf{s}_r(t)+\mathbf{n}(t), \tag{4}$$

where $\mathbf{\Phi}=\mathrm{diag}(e^{j\varphi_1},\ldots,e^{j\varphi_Q})$,, in which φ_p denotes the arbitrary and possibly unknown initial phase of the pth signal, and it is assumed that $e^{j\varphi_p}\neq e^{j\varphi_q}$ for any $p\neq q$. In addition, $\mathbf{s}_r(t)$ in (4) is the real signal vector, that is, $s_r^*(t)=\mathbf{s}_r(t)$, where * denotes conjugate. In the sequel, we will specialize in direction-finding for $Q<4$ signals satisfying model (4).

It is further assumed that all the signals are statistical independent and have nonzero fourth-order cumulant (and hence nonzero conjugate fourth-order cumulant [17]), that is

$$\begin{cases}\mathrm{Cum}(s_p(t),\ s_p^*(t),\ s_p(t),s_p^*(t))\neq 0,\\ \mathrm{Cum}(s_p(t),\ s_p^*(t),\ s_p(t),\ s_p(t))\neq 0,\end{cases}\ p=1,2,\ldots,Q.$$

We next define the cleaned array covariance matrix as

$$\mathbf{R}_x\overset{\text{def}}{=}E(\mathbf{x}(t)\mathbf{x}^{\mathrm{H}}(t))-\sigma_n^2\mathbf{I}=\mathbf{A}\mathbf{R}_s\mathbf{A}^{\mathrm{H}} \tag{5}$$

the conjugate array covariance matrix as (note $\mathbf{A}$ is a real matrix)

$$\mathbf{R}_{x^*}\overset{\text{def}}{=}E(\mathbf{x}(t)\mathbf{x}^{\mathrm{T}}(t))=\mathbf{A}\mathbf{R}_{s^*}\mathbf{A}^{\mathrm{H}}=\mathbf{A}\mathbf{R}_s\mathbf{\Phi}^2\mathbf{A}^{\mathrm{H}}, \tag{6}$$

where $\mathbf{R}_s\overset{\text{def}}{=}E(\mathbf{s}(t)\mathbf{s}^{\mathrm{H}}(t))=\mathbf{\Phi}\mathbf{R}_{r,s}\mathbf{\Phi}^{\mathrm{H}}$, $\mathbf{R}_{r,s}\overset{\text{def}}{=}E(\mathbf{s}_r(t)\mathbf{s}_r^{\mathrm{H}}(t))$, and $\mathbf{R}_{s^*}=\mathbf{\Phi}\mathbf{R}_{r,s}\mathbf{\Phi}^{\mathrm{T}}=\mathbf{R}_s\mathbf{\Phi}^2$. We then eigendecompose $\mathbf{R}_x$ to obtain $\mathbf{R}_x=\mathbf{E}_s\mathbf{\Sigma}_s\mathbf{E}_s^{\mathrm{H}}+0\cdot\mathbf{E}_n\mathbf{E}_n^{\mathrm{H}}$, and compute $\mathbf{P}_n=\mathbf{E}_n\mathbf{E}_n^{\mathrm{H}}$, where $\mathbf{E}_s$ and $\mathbf{E}_n$ are the signal matrix and noise matrix containing the Q principal eigenvectors (associated with the Q largest eigenvalues) and the

$4-Q$ subordinate eigenvectors (associated with the $4-Q$ smallest eigenvalues), respectively. $\mathbf{\Sigma}_s$ is a diagonal matrix whose diagonal entries are the Q largest eigenvalues of $\mathbf{R}_x$.

We further define the following nonconjugate and conjugate fourth-order cumulant matrices (we refer the reader to [17] for the detailed definitions and properties of cumulant computation):

$$\begin{aligned}\mathbf{C}_m &= \mathrm{Cum}(x_m(t), x_m^*(t), \mathbf{x}(t), \mathbf{x}^{\mathrm{H}}(t)) \\ &= \sum_{p=1}^{Q} \underbrace{\left[|a_{p,m}|^2 \mathrm{Cum}(s_p(t), s_p^*(t), s_p(t), s_p^*(t))\right]}_{\stackrel{\mathrm{def}}{=} \varsigma'_{p,m}} \mathbf{a}_p \mathbf{a}_p^{\mathrm{H}} \\ &= \mathbf{A}\mathbf{\Lambda}_m \mathbf{A}^{\mathrm{H}} \end{aligned} \tag{7}$$

and

$$\begin{aligned}\mathbf{D}_m &= \mathrm{Cum}(x_m(t), x_m^*(t), \mathbf{x}(t), \mathbf{x}^{\mathrm{T}}(t)) \\ &= \sum_{p=1}^{Q} \left[|a_{p,m}|^2 e^{j2\varphi_p} \mathrm{Cum}(s_p(t), s_p^*(t), s_p(t), s_p^*(t))\right] \mathbf{a}_p \mathbf{a}_p^{\mathrm{H}} \\ &= \mathbf{A}\mathbf{\Lambda}_m \mathbf{\Phi}^2 \mathbf{A}^{\mathrm{H}}, \end{aligned} \tag{8}$$

where $\mathbf{\Lambda}_m = \mathrm{diag}(\varsigma'_{1,m}, \ldots, \varsigma'_{Q,m})$, $x_m(t)$ and $a_{p.m}$ are the mth element of $\mathbf{x}(t)$ and $\mathbf{a}_p$, respectively.

In practice, $\mathbf{R}_x$, $\mathbf{R}_{x^*}$, $\mathbf{C}_m$ and $\mathbf{D}_m$ defined in (5)–(8) have to be estimated from undersampled independent discrete-time data samples (for oversampled data samples, cyclostationarity of noncircular signals may also be taken into account to blindly separate those incident sources with distinct cyclic frequencies [18], which, however, is quite different from our method to be described below), that is,

$$\widehat{\mathbf{R}}_x = \frac{1}{K}\left(\sum_{k=1}^{K} \mathbf{x}(t_k)\mathbf{x}^{\mathrm{H}}(t_k)\right) - \widehat{\sigma}_n^2 \mathbf{I}, \tag{9}$$

$$\widehat{\mathbf{R}}_{x^*} = \frac{1}{K}\sum_{k=1}^{K} \mathbf{x}(t_k)\mathbf{x}^{\mathrm{T}}(t_k), \tag{10}$$

$$\begin{aligned}\widehat{\mathbf{C}}_m = &\left(\frac{K+2}{K^2-K}\right)\sum_{k=1}^{K} x_m(t_k)x_m^*(t_k)\mathbf{x}(t_k)\mathbf{x}^{\mathrm{H}}(t_k) \\ &- \left(\frac{1}{K^2-K}\right)\left(\sum_{k=1}^{K} x_m(t_k)x_m^*(t_k)\right)\left(\sum_{k=1}^{K} \mathbf{x}(t_k)\mathbf{x}^{\mathrm{H}}(t_k)\right) \\ &- \left(\frac{1}{K^2-K}\right)\left(\sum_{k=1}^{K} x_m(t_k)\mathbf{x}(t_k)\right)\left(\sum_{k=1}^{K} x_m^*(t_k)\mathbf{x}^{\mathrm{H}}(t_k)\right) \\ &- \left(\frac{1}{K^2-K}\right)\left(\sum_{k=1}^{K} x_m^*(t_k)\mathbf{x}(t_k)\right)\left(\sum_{k=1}^{K} x_m(t_k)\mathbf{x}^{\mathrm{H}}(t_k)\right). \end{aligned} \tag{11}$$

$$\begin{aligned}\widehat{\mathbf{D}}_m = &\left(\frac{K+2}{K^2-K}\right)\sum_{k=1}^{K} x_m(t_k)x_m^*(t_k)\mathbf{x}(t_k)\mathbf{x}^{\mathrm{T}}(t_k), \\ &- \left(\frac{1}{K^2-K}\right)\left(\sum_{k=1}^{K} x_m(t_k)x_m^*(t_k)\right)\left(\sum_{k=1}^{K} \mathbf{x}(t_k)\mathbf{x}^{\mathrm{T}}(t_k)\right), \\ &- \left(\frac{1}{K^2-K}\right)\left(\sum_{k=1}^{K} x_m(t_k)\mathbf{x}(t_k)\right)\left(\sum_{k=1}^{K} x_m^*(t_k)\mathbf{x}^{\mathrm{T}}(t_k)\right), \\ &- \left(\frac{1}{K^2-K}\right)\left(\sum_{k=1}^{K} x_m^*(t_k)\mathbf{x}(t_k)\right)\left(\sum_{k=1}^{K} x_m(t_k)\mathbf{x}^{\mathrm{T}}(t_k)\right), \end{aligned} \tag{12}$$

where $\{x(t_k)\}_{k=1}^{K}$ are the available data samples, K is the number of snapshot, $\widehat{\sigma}_n^2$ is an estimate of σ_n^2 which may be obtained as follows [24]:

$$\widehat{\sigma}_n^2 = \frac{1}{4-Q}\sum_{k=Q+1}^{4}\widehat{v}_k, \tag{13}$$

where $\{\widehat{v}_k\}_{k=Q+1}^{4}$ are the $4-Q$ smallest eigenvalues of the sample covariance matrix $\widehat{\underline{\mathbf{R}}}_x = K^{-1}\sum_{k=1}^{K}\mathbf{x}(t_k)\mathbf{x}^{\mathrm{H}}(t_k)$. Let $\mathbf{v}_{L,k}$ and $\mathbf{v}_{\mathrm{R},k}$, respectively, be the left and right eigenvectors associated with v_k (the true value of $\widehat{v}_k$, i.e., the kth eigenvalue of the true array covariance matrix $\underline{\mathbf{R}}_x = E(\mathbf{x}(t)\mathbf{x}^{\mathrm{H}}(t))$), then from [23] we have $\Delta v_k = \widehat{v}_k - v_k \simeq \mathbf{v}_{L,k}\Delta\underline{\mathbf{R}}_x\mathbf{v}_{R,k}$, where $k = Q+1,\ldots,4$, and $\Delta\underline{\mathbf{R}}_x = \widehat{\underline{\mathbf{R}}}_x - \underline{\mathbf{R}}_x$. Note that $E(\widehat{\underline{\mathbf{R}}}_x) = K^{-1}\sum_{k=1}^{K} E(\mathbf{x}(t_k)\mathbf{x}^{H}(t_k)) = \underline{\mathbf{R}}_x$, we then have $E(\widehat{v}_k) = v_k$, and therefore $E(\widehat{\sigma}_n^2) = \sigma_n^2$.

3. Two types of conjugate MI-ESPRIT algorithms

3.1. Regularization formulation of ESPRIT

The matrix pencil required by ESPRIT implementation herein is defined as follows:

$$\{\mathbf{M}_1, \mathbf{M}_2\} = \{\mathbf{AH}, \mathbf{A\Sigma H}\}, \tag{14}$$

where $\mathbf{H}$ is a matrix of full rank, $\mathbf{\Sigma}$ is a $Q\times Q$ diagonal matrix whose diagonal entries may contain the desired parameter information such as DOAs. From matrix knowledge, there must exist a 4×4 matrix $\mathbf{\Psi} = \{\psi(m,l)\}_{m,l=1}^{4}$ such that $\mathbf{\Psi AH} = \mathbf{A\Sigma H}$ and, hence $\mathbf{\Psi A} = \mathbf{A\Sigma}$. Therefore, $\mathbf{\Psi} = \mathbf{A\Sigma A}^{+} + \mathscr{R}(\mathbf{I}_4 - \mathbf{AA}^{+})$, where $\mathbf{A}^{+} = (\mathbf{A}^{\mathrm{H}}\mathbf{A})^{-1}\mathbf{A}^{\mathrm{H}}$ is the left pseudo-inverse of $\mathbf{A}$, $\mathscr{R}$ is a matrix with arbitrary elements. Among all the possible solutions to the underdetermined equation system $\mathbf{\Psi AH} = \mathbf{A\Sigma H}$ or $\mathbf{\Psi A} = \mathbf{A\Sigma}$, $\mathbf{\Psi}_{\mathrm{MN}} = \mathbf{A\Sigma A}^{+}$ has the smallest Frobenius norm, since, for $\forall\mathbf{\Psi}$ satisfying $\mathbf{\Psi A} = \mathbf{A\Sigma}$, we have

$$\begin{aligned}||\mathbf{\Psi}||_F^2 &= ||\mathbf{\Psi}_{\mathrm{MN}} + \mathbf{\Psi} - \mathbf{\Psi}_{\mathrm{MN}}||_F^2 \\ &= ||\mathbf{\Psi}_{\mathrm{MN}}||_F^2 + ||\mathbf{\Psi} - \mathbf{\Psi}_{\mathrm{MN}}||_F^2 + 2\mathrm{Re}\{\mathrm{trace}[(\mathbf{\Psi} - \mathbf{\Psi}_{\mathrm{MN}})\mathbf{\Psi}_{\mathrm{MN}}^{\mathrm{H}}]\},\end{aligned} \tag{15}$$

where $||\cdot||_F$ denotes the Frobenius norm. In addition, $\mathbf{\Psi}_{\mathrm{MN}} = \mathbf{A\Sigma A}^{+} = \mathbf{\Psi}\mathrm{AA}^{+}$, hence

$$(\mathbf{\Psi} - \mathbf{\Psi}_{\mathrm{MN}})\mathbf{\Psi}_{\mathrm{MN}}^{\mathrm{H}} = \mathbf{\Psi}(\mathbf{I} - \mathbf{AA}^{+})\mathbf{A}(\mathbf{A}^{\mathrm{H}}\mathbf{A})^{-1}\mathbf{\Sigma}^{\mathrm{H}}\mathbf{A}^{\mathrm{H}} = \mathbf{O}, \tag{16}$$

which means $||\mathbf{\Psi}||_F^2 = ||\mathbf{\Psi}_{\mathrm{MN}}||_F^2 + ||\mathbf{\Psi} - \mathbf{\Psi}_{\mathrm{MN}}||_F^2$, and then $||\mathbf{\Psi}||_F^2 \geqslant ||\mathbf{\Psi}_{\mathrm{MN}}||_F^2$. Based on the above observations, $\mathbf{\Psi}_{\mathrm{MN}}$ may be obtained as follows:

$$\min_{\mathbf{\Psi}} ||\mathbf{\Psi M}_1 - \mathbf{M}_2||_F^2 + \kappa'||\mathbf{\Psi}||_F^2, \tag{17}$$

wherein $\kappa' \to 0$ (in fact, as $\kappa' \to 0$, (17) is equivalent to {minimizing $||\mathbf{\Psi}||_F^2$, subject to $\mathbf{\Psi M}_1 = \mathbf{M}_2$}). Furthermore, since $(\mathbf{I} - \mathbf{AA}^{+})\mathbf{\Psi}_{\mathrm{MN}} = \mathbf{O}$, $\mathbf{\Psi}_{\mathrm{MN}}$ may also be obtained as follows:

$$\min_{\mathbf{\Psi}} ||\mathbf{\Psi M}_1 - \mathbf{M}_2||_F^2 + \kappa''||\mathbf{P}_n\mathbf{\Psi}||_F^2, \tag{18}$$

where $\mathbf{P}_n = \mathbf{I} - \mathbf{AA}^{+}$, $\kappa'' \neq 0$. In the above, κ' and κ'' are often called the regularization parameters.

From Section 2, we may obtain the following multiple matrix pencils required by MI-ESPRIT implementation:

$$\left.\begin{aligned}&\{(\mathbf{R}_x)^{\mathrm{H}} = \mathbf{AR}_s\mathbf{A}^{\mathrm{H}},\ (\mathbf{R}_{x^*})^{\mathrm{H}} = \mathbf{A\Phi}^{-2}\mathbf{R}_s\mathbf{A}^{\mathrm{H}}\},\\ &\{(\mathbf{C}_m)^{\mathrm{H}} = \mathbf{A\Lambda}_m^{\mathrm{H}}\mathbf{A}^{\mathrm{H}},\ (\mathbf{D}_m)^{\mathrm{H}} = \mathbf{A\Phi}^{-2}\mathbf{\Lambda}_m^{\mathrm{H}}\mathbf{A}^{\mathrm{H}}\},\ m = 1,\ 2,\ 3,\ 4.\end{aligned}\right\} \tag{19}$$

As has mentioned earlier, there exists a matrix $\mathbf{\Pi} = \mathbf{A\Phi}^{-2}\mathbf{A}^{+}$ such that $\mathbf{\Pi}(\mathbf{R}_x)^{\mathrm{H}} = (\mathbf{R}_{x^*})^{\mathrm{H}}$, $\mathbf{\Pi}(\mathbf{C}_m)^{\mathrm{H}} = (\mathbf{D}_m)^{\mathrm{H}}$, where $m = 1,2,3,4$, and the major step in the proposed conjugate MI-ESPRIT then is focused on calculating this target matrix $\mathbf{\Pi}$. Since $\mathbf{\Pi A} = \mathbf{A\Phi}^{-2}$, and $\mathrm{rank}(\mathbf{\Pi}) = Q$, it is seen that the pth principal eigenvector ε_p associated with nonzero eigenvalue of $\mathbf{\Pi}$ represents a scaled version of the pth steering vector $\mathbf{a}_p$, that is, $\varepsilon_p = \zeta'\mathbf{a}_p$, where ζ' is a scalar, and $p = 1,2,\ldots,Q$. Then, DOA estimates can be obtained from $\{\varepsilon_p\}_{p=1}^{Q}$ since $\mathbf{a}_p$

contains all necessary information for unambiguous localization. For clarity, in the sequel, we will call the target matrix $\mathbf{\Pi}$ the ESPRIT matrix, which is the object of the provided asymptotic perturbation analyses.

Unfortunately, the ESPRIT matrix $\mathbf{\Pi}$ is only one of the nonunique solutions to the next ill-posed equation system:

$$\begin{aligned}\mathbf{X}(\mathbf{R}_x)^{\mathrm{H}} &= (\mathbf{R}_{x^*})^{\mathrm{H}}\\ &\Rightarrow \mathbf{X}[\mathbf{A}(\mathbf{R}_s^{\mathrm{H}}\mathbf{A}^{\mathrm{H}})] = \mathbf{A}\mathbf{\Phi}^{-2}(\mathbf{R}_s^{\mathrm{H}}\mathbf{A}^{\mathrm{H}})\\ &\Rightarrow \mathbf{X}\mathbf{A} = \mathbf{A}\mathbf{\Phi}^{-2}\end{aligned} \tag{20}$$

or

$$\begin{aligned}\mathbf{X}(\mathbf{C}_m)^{\mathbf{H}} &= (\mathbf{D}_m)^{\mathrm{H}}\\ &\Rightarrow \mathbf{X}[\mathbf{A}(\mathbf{\Lambda}_m^{\mathrm{H}}\mathbf{A}^{\mathrm{H}})] = \mathbf{A}\mathbf{\Phi}^{-2}(\mathbf{\Lambda}_m^{\mathrm{H}}\mathbf{A}^{\mathrm{H}})\\ &\Rightarrow \mathbf{X}\mathbf{A} = \mathbf{A}\mathbf{\Phi}^{-2},\end{aligned} \tag{21}$$

where $m = 1,2,3,4$. To exhaust the inherent degree-of-freedom (DOF) in the above problems, two schemes motivated by (17) and (18) are suggested in the conjugate MI-ESPRIT, as briefly described below. The proposed two schemes may be viewed as the least-squares simplifications of the standard MI-ESPRIT [19], and both explore the redundancies in the nonzero conjugate moments, hence the name conjugate MI-ESPRIT. Before proceeding, we remark that in practice the data statistics used in the above systems should be replaced by their sample versions given in (9)–(12), and then using (17) and (18) may not always obtain the desired solution $\mathbf{\Psi}_{\mathrm{MN}}$. Although $\widehat{\mathbf{R}}_x$ and $\widehat{\mathbf{C}}_m$ will generally become full rank due to perturbation, the problem is still ill-posed since $\widehat{\mathbf{R}}_x$ and $\widehat{\mathbf{C}}_m$ are very near singular and hence results in an unstable solution. Thus, some appropriate constraints should be incorporated to smooth the solution, a slightly different attempt from DOF reduction. For exposition convenience, we define $\mathbf{\Xi} = \mathbf{\Pi}^{\mathrm{H}} \stackrel{\mathrm{def}}{=} \check{\mathbf{\Pi}}$, thus $\mathbf{R}_x\mathbf{\Xi} = \mathbf{R}_{x^*}$, $\mathbf{C}_m\mathbf{\Xi} = \mathbf{D}_m$, and both of our proposals are then concentrated on calculating $\mathbf{\Xi}$ instead of $\mathbf{\Pi}$.

3.2. Norm-penalized conjugate MI-ESPRIT

The norm-penalized conjugate MI-ESPRIT suggests to solve the following problem:

$$\min_{\mathbf{\Xi}} \kappa||\mathbf{\Xi}||_F^2 + ||\widehat{\mathbf{R}}_x\mathbf{\Xi} - \widehat{\mathbf{R}}_{x^*}||_F^2 + \lambda\sum_{m=1}^{4}||\widehat{\mathbf{C}}_m\mathbf{\Xi} - \widehat{\mathbf{D}}_m||_F^2, \tag{22}$$

where $\kappa > 0$ is the regularization parameter, $\lambda > 0$ is a whitening-factor for balancing the perturbations in the second-order statistics (SOS) term and the higher-order statistics (HOS) term.

Note that (22) is equivalent to the next linear least-squares problem:

$$\min_{\mathbf{\Xi}} \left\| \underbrace{\begin{pmatrix} \sqrt{\kappa}\mathbf{I} \\ \widehat{\mathbf{R}}_x \\ \sqrt{\lambda}\widehat{\mathbf{C}}_1 \\ \vdots \\ \sqrt{\lambda}\widehat{\mathbf{C}}_4 \end{pmatrix}}_{\stackrel{\mathrm{def}}{=}\widehat{\mathbf{F}}_1} \mathbf{\Xi} - \underbrace{\begin{pmatrix} \mathbf{O} \\ \widehat{\mathbf{R}}_{x^*} \\ \sqrt{\lambda}\widehat{\mathbf{D}}_1 \\ \vdots \\ \sqrt{\lambda}\widehat{\mathbf{D}}_4 \end{pmatrix}}_{\stackrel{\mathrm{def}}{=}\widehat{\mathbf{F}}_2} \right\|_F^2. \tag{23}$$

Let "vec($\mathbf{X}$)" denote a vector-valued function that maps an $M \times N$ matrix "$\mathbf{X}$" into an MN-dimensional column vector by just stacking the columns of $\mathbf{X}$, (23) is further equivalent to

$$\min_{\mathbf{\Xi}} ||\mathrm{vec}(\widehat{\mathbf{F}}_1\mathbf{\Xi}\mathbf{I}) - \mathrm{vec}(\widehat{\mathbf{F}}_2)||_2^2 \Rightarrow \min_{\mathbf{\Xi}} ||(\mathbf{I}\otimes\widehat{\mathbf{F}}_1)\mathrm{vec}(\mathbf{\Xi}) - \mathrm{vec}(\widehat{\mathbf{F}}_2)||_2^2, \tag{24}$$

where "⊗" denotes Kronecker product, $||\cdot||_2$ denotes Euclid-norm. The solution to (24) amounts to finding the least squares solution to $(\mathbf{I}\otimes\widehat{\mathbf{F}}_1)\mathrm{vec}(\mathbf{\Xi})=\mathrm{vec}(\widehat{\mathbf{F}}_2)$, and hence

$$\begin{aligned}(\mathrm{vec}(\Xi))_{LS} &= [(\mathbf{I}\otimes\widehat{\mathbf{F}}_1)^{\mathrm{H}}(\mathbf{I}\otimes\widehat{\mathbf{F}}_1)]^{-1}(\mathbf{I}\otimes\widehat{\mathbf{F}}_1)^{\mathrm{H}}\mathrm{vec}(\widehat{\mathbf{F}}_2)\\ &= [\mathbf{I}\otimes((\widehat{\mathbf{F}}_1^{\mathrm{H}}\widehat{\mathbf{F}}_1)^{-1}\widehat{\mathbf{F}}_1^{\mathrm{H}})]\mathrm{vec}(\widehat{\mathbf{F}}_2)\\ &= [\mathbf{I}\otimes(\widehat{\mathbf{F}}_1^{+})]\mathrm{vec}(\widehat{\mathbf{F}}_2)\end{aligned} \tag{25}$$

Then, the least-squares-type solution to (22) is finally given by

$$\begin{aligned}\widehat{\mathbf{\Xi}}_{\mathrm{NP}} &= \widehat{\mathbf{F}}_1^{+}\widehat{\mathbf{F}}_2=(\widehat{\mathbf{F}}_1^{\mathrm{H}}\widehat{\mathbf{F}}_1)^{-1}\widehat{\mathbf{F}}_1^{\mathrm{H}}\widehat{\mathbf{F}}_2\\ &= \left(\kappa\mathbf{I}+\widehat{\mathbf{R}}_x^{\mathrm{H}}\widehat{\mathbf{R}}_x+\lambda\sum_{m=1}^{4}\widehat{\mathbf{C}}_m^{\mathrm{H}}\widehat{\mathbf{C}}_m\right)^{-1}\left(\widehat{\mathbf{R}}_x^{\mathrm{H}}\widehat{\mathbf{R}}_{x^*}+\lambda\sum_{m=1}^{4}\widehat{\mathbf{C}}_m^{\mathrm{H}}\widehat{\mathbf{D}}_m\right).\end{aligned} \tag{26}$$

Next, we may eigendecompose $\widehat{\mathbf{\Xi}}_{NP}^{\mathrm{H}}$ to obtain the Q principal eigenvectors $\widehat{\varepsilon}_p$, and then estimate the steering vector $\mathbf{a}_p$ as $\widehat{\mathbf{a}}_p=\widehat{\varepsilon}_p/\widehat{\varepsilon}_p(4)$, from which DOAs of signals can be ultimately obtained.

3.3. Subspace-constraint conjugate MI-ESPRIT

The subspace-constraint conjugate MI-ESPRIT proposes to solve the following problem (recalling that $\mathbf{P}_n\mathbf{\Xi}=\mathbf{O}$):

$$\min_{\mathbf{\Xi}}\kappa||\widehat{\mathbf{P}}_n\mathbf{\Xi}||_F^2+\ ||\widehat{\mathbf{R}}_x\mathbf{\Xi}-\widehat{\mathbf{R}}_{x^*}||_F^2+\ \lambda\sum_{m\ =\ 1}^{4}||\widehat{\mathbf{C}}_m\mathbf{\Xi}-\widehat{\mathbf{D}}_m||_F^2, \tag{27}$$

where $\widehat{\mathbf{P}}_n$ is an estimate of $\mathbf{P}_n$, for example, $\widehat{\mathbf{P}}_n=\widehat{\mathbf{U}}_n\widehat{\mathbf{U}}_n^{\mathrm{H}}$ with $\widehat{\mathbf{U}}_n$ denoting the noise matrix of $\widehat{\mathbf{R}}_x$. Note that (27) amounts to solving the next linear least-squares problem:

$$\min_{\mathbf{\Xi}}\left\|\underbrace{\begin{pmatrix}\sqrt{\kappa}\widehat{\mathbf{P}}_n\\ \widehat{\mathbf{R}}_x\\ \sqrt{\lambda}\widehat{\mathbf{C}}_1\\ \vdots\\ \sqrt{\lambda}\widehat{\mathbf{C}}_4\end{pmatrix}}_{\stackrel{\mathrm{def}}{=}\widehat{\mathbf{H}}_1}\mathbf{\Xi}-\begin{pmatrix}\mathbf{O}\\ \widehat{\mathbf{R}}_{x^*}\\ \sqrt{\lambda}\widehat{\mathbf{D}}_1\\ \vdots\\ \sqrt{\lambda}\widehat{\mathbf{D}}_4\end{pmatrix}\right\|_F^2. \tag{28}$$

The solution to (27) thus is given by (similar to Section 3.2)

$$\begin{aligned}\widehat{\mathbf{\Xi}}_{\mathrm{SC}} &= \widehat{\mathbf{H}}_1^{+}\widehat{\mathbf{F}}_2=(\widehat{\mathbf{H}}_1^{\mathrm{H}}\widehat{\mathbf{H}}_1)^{-1}\widehat{\mathbf{H}}_1\widehat{\mathbf{H}}_2\\ &= \left(\kappa\widehat{\mathbf{P}}_n+\widehat{\mathbf{R}}_x^{\mathrm{H}}\widehat{\mathbf{R}}_x+\lambda\sum_{m=1}^{4}\widehat{\mathbf{C}}_m^{\mathrm{H}}\widehat{\mathbf{C}}_m\right)^{-1}\left(\widehat{\mathbf{R}}_x^{\mathrm{H}}\widehat{\mathbf{R}}_{x*}+\lambda\sum_{m=1}^{4}\widehat{\mathbf{C}}_m^{\mathrm{H}}\widehat{\mathbf{D}}_m\right).\end{aligned} \tag{29}$$

We then eigendecompose $\widehat{\mathbf{\Xi}}_{\mathrm{SC}}^{\mathrm{H}}$ to obtain the Q principal eigenvectors $\widehat{\varepsilon}_p'$, and estimate $\mathbf{a}_p$ as $\widehat{\mathbf{a}}_p=\widehat{\varepsilon}_p'/\widehat{\varepsilon}_p'(4)$.

If we replace $\widehat{\mathbf{P}}_n$, $\widehat{\mathbf{R}}_x$, $\widehat{\mathbf{R}}_{x^*}$, $\widehat{\mathbf{C}}_m$ and $\widehat{\mathbf{D}}_m$ by $\mathbf{P}_n$, $\mathbf{R}_x$, $\mathbf{R}_{x^*}$, $\mathbf{C}_m$ and $\mathbf{D}_m$ in the above solutions given by (26) and (29), then $\widehat{\mathbf{\Xi}}_{\mathrm{NP}}(\kappa\to 0)=\widehat{\mathbf{\Xi}}_{\mathrm{SC}}(\kappa\neq 0)=(\mathbf{A}\mathbf{\Phi}^{-2}\mathbf{A}^{+})^{\mathrm{H}}\stackrel{\mathrm{def}}{=}\check{\mathbf{\Pi}}$. In the presence of noisy $\widehat{\mathbf{P}}_n$, $\widehat{\mathbf{R}}_n$, $\widehat{\mathbf{R}}_{x^*}$, $\widehat{\mathbf{C}}_m$ and $\widehat{\mathbf{D}}_m$, on the other hand, $\widehat{\mathbf{\Xi}}_{\mathrm{NP}}(\kappa\to 0)$ and $\widehat{\mathbf{\Xi}}_{\mathrm{SC}}(\kappa\neq 0)$ generally deviates from $\check{\mathbf{\Pi}}$. In the sequel, we will provide the perturbation analyses on $\widehat{\mathbf{\Xi}}_{\mathrm{NP}}$ and $\widehat{\mathbf{\Xi}}_{\mathrm{SC}}$ in terms of bias and mean-squared error.

4. Perturbation analysis of the norm-penalized ESPRIT matrix

4.1. Bias analysis

Recall that (22) is equivalent to the next linear LSF problem:

$$\min_{\boldsymbol{\Xi}} \left\| \begin{pmatrix} \sqrt{\kappa}\mathbf{I} \\ \widehat{\mathbf{R}}_x \\ \sqrt{\lambda}\widehat{\mathbf{C}}_1 \\ \vdots \\ \sqrt{\lambda}\widehat{\mathbf{C}}_4 \end{pmatrix} \boldsymbol{\Xi} - \begin{pmatrix} \mathbf{O} \\ \widehat{\mathbf{R}}_{x^*} \\ \sqrt{\lambda}\widehat{\mathbf{D}}_1 \\ \\ \sqrt{\lambda}\widehat{\mathbf{D}}_4 \end{pmatrix} \right\|_F^2 = \min_{\boldsymbol{\Xi}} ||\widehat{\mathbf{F}}_1\boldsymbol{\Xi} - \widehat{\mathbf{F}}_2||_F^2. \tag{30}$$

Let $\Delta\boldsymbol{\Xi}_{\mathrm{NP}} = \widehat{\boldsymbol{\Xi}}_{\mathrm{NP}} - \check{\boldsymbol{\Pi}}$, $\Delta\mathbf{F}_1 = \widehat{\mathbf{F}}_1 - \mathbf{F}_1$, and $\Delta\mathbf{F}_2 = \widehat{\mathbf{F}}_2 - \mathbf{F}_2$. Then, $(\mathbf{F}_1 + \Delta\mathbf{F}_1)(\check{\boldsymbol{\Pi}} + \Delta\boldsymbol{\Xi}_{\mathrm{NP}}) \simeq \mathbf{F}_2 + \Delta\mathbf{F}_2$, and therefore (using, in turn, $\mathbf{F}_1\check{\boldsymbol{\Pi}} = \mathbf{F}_2 + \boldsymbol{\Omega}$, where $\boldsymbol{\Omega} = [\sqrt{\kappa}\check{\boldsymbol{\Pi}}^{\mathrm{T}}, \mathbf{O}_{4,20}]^{\mathrm{T}}$, and $\Delta\mathbf{F}_1\Delta\boldsymbol{\Xi}_{\mathrm{NP}} \simeq \mathrm{O}$)

$$\begin{aligned} \Delta\boldsymbol{\Xi}_{\mathrm{NP}} \simeq (\mathbf{F}_1^{\mathrm{H}}\mathbf{F}_1)^{-1}\mathbf{F}_1^{\mathrm{H}}(\Delta\mathbf{F}_2 - \Delta\mathbf{F}_1\check{\boldsymbol{\Pi}} - \boldsymbol{\Omega}) = & -\left(\kappa\mathbf{I} + \underbrace{\mathbf{R}_x^{\mathrm{H}}\mathbf{R}_x + \lambda\sum_{m=1}^{4}\mathbf{C}_m^{\mathrm{H}}\mathbf{C}_m}_{\stackrel{\mathrm{def}}{=}\mathbf{G}}\right)^{-1} \\ & \times \left[\underbrace{\left(\mathbf{R}_x^{\mathrm{H}}(\Delta\mathbf{R}_x\check{\boldsymbol{\Pi}} - \Delta\mathbf{R}_{x^*}) + \lambda\sum_{m=1}^{4}\mathbf{C}_m^{\mathrm{H}}(\Delta\mathbf{C}_m\check{\boldsymbol{\Pi}} - \Delta\mathbf{D}_m)\right)}_{\stackrel{\mathrm{def}}{=}\Delta\mathbf{U}} + \kappa\check{\boldsymbol{\Pi}}\right] \\ = & -(\kappa\mathbf{I} + \mathbf{G})^{-1}(\Delta\mathbf{U} + \kappa\check{\boldsymbol{\Pi}}), \end{aligned} \tag{31}$$

where $\Delta\mathbf{R}_{x^*} = \widehat{\mathbf{R}}_{x^*} - \mathbf{R}_{x^*}$, $\Delta\mathbf{R}_x = \widehat{\mathbf{R}}_x - \mathbf{R}_x$, $\Delta\mathbf{C}_m = \widehat{\mathbf{C}}_m - \mathbf{C}_m$, $\Delta\mathbf{D}_m = \widehat{\mathbf{D}}_m - \mathbf{D}_m$, and $\boldsymbol{\Omega} = [\sqrt{\kappa}\widehat{\boldsymbol{\Pi}}^{\mathrm{T}}, \mathbf{O}_{4,20}]^{\mathrm{T}}$. From (9) we have

$$E(\widehat{\mathbf{R}}_x) = \frac{1}{K}\sum_{k=1}^{K}E(\mathbf{x}(t_k)\mathbf{x}^{\mathrm{H}}(t_k)) - E(\widehat{\sigma}_n^2)\mathbf{I} = \frac{1}{K}\sum_{k=1}^{K}\underline{\mathbf{R}}_x - \sigma_n^2\mathbf{I} = \mathbf{R}_x \tag{32}$$

and hence $E(\Delta\mathbf{R}_x) = E(\widehat{\mathbf{R}}_x) - \mathbf{R}_x = \mathbf{O}$. Similarly, $E(\widehat{\mathbf{R}}_{x^*}) = K^{-1}\sum_{k=1}^{K}E(\mathbf{x}(t_k)\mathbf{x}^{\mathrm{T}}(t_k)) = \mathbf{R}_{x^*}$, and $E(\Delta\mathbf{R}_{x^*}) = \mathbf{O}$. In addition, from (11), the (i,j)th element of $\widehat{\mathbf{C}}_m$ is given by

$$\begin{aligned} \widehat{\mathbf{C}}_m(i,j) = & \frac{K+2}{K^2-K}\sum_{k=1}^{K}x_m(t_k)x_m^*(t_k)x_i(t_k)x_j^*(t_k) \\ & - \frac{1}{K^2-K}\sum_{k_1=1}^{K}\sum_{k_2=1}^{K}x_m(t_{k_1})x_m^*(t_{k_1})x_i(t_{k_2})x_j^*(t_{k_2}) \\ & - \frac{1}{K^2-K}\sum_{k_1=1}^{K}\sum_{k_2=1}^{K}x_m(t_{k_1})x_i(t_{k_1})x_m^*(t_{k_2})x_j^*(t_{k_2}) \\ & - \frac{1}{K^2-K}\sum_{k_1=1}^{K}\sum_{k_2=1}^{K}x_m(t_{k_1})x_j^*(t_{k_1})x_m^*(t_{k_2})x_i(t_{k_2}). \end{aligned} \tag{33}$$

Recall that $x_m(t_{k_1})$ is independent of $x_n(t_{k_2})$ for $t_{k_1} \neq t_{k_2}$. Then we have

$$\begin{aligned}
E(\widehat{\mathbf{C}}_m(i,j)) &= \frac{K+2}{K^2-K}\sum_{k=1}^{K} E(x_m(t_k)x_m^*(t_k)x_i(t_k)x_j^*(t_k)) \\
&\quad - \frac{1}{K^2-K}\sum_{k_1=1}^{K}\sum_{k_2=1}^{K} E(x_m(t_{k_1})x_m^*(t_{k_1})x_i(t_{k_2})x_j^*(t_{k_2})) \\
&\quad - \frac{1}{K^2-K}\sum_{k_1=1}^{K}\sum_{k_2=1}^{K} E(x_m(t_{k_1})x_i(t_{k_1})x_m^*(t_{k_2})x_j^*(t_{k_2})) \\
&\quad - \frac{1}{K^2-K}\sum_{k_1=1}^{K}\sum_{k_2=1}^{K} E(x_m(t_{k_1})x_j^*(t_{k_1})x_m^*(t_{k_2})x_i(t_{k_2})) \\
&= \frac{(K+2)K}{K^2-K} E(x_m(t)x_m^*(t)x_i(t)x_j^*(t)) \\
&\quad - \frac{3}{K^2-K}\sum_{k=1}^{K} E(x_m(t_{k_1})x_m^*(t_{k_1})x_i(t_{k_2})x_j^*(t_{k_2})) \\
&\quad - \frac{1}{K^2-K}\sum_{k_1,k_2=1,k_1\neq k_2}^{K} E(x_m(t_{k_1})x_m^*(t_{k_1}))E(x_i(t_{k_2})x_j^*(t_{k_2})) \\
&\quad - \frac{1}{K^2-K}\sum_{k_1,k_2=1,k_1\neq k_2}^{K} E(x_m(t_{k_1})x_i(t_{k_1}))E(x_m^*(t_{k_2})x_j^*(t_{k_2})) \\
&\quad - \frac{1}{K^2-K}\sum_{k_1,k_2=1,k_1\neq k_2}^{K} E(x_m(t_{k_1})x_j^*(t_{k_1}))E(x_m^*(t_{k_2})x_i(t_{k_2})) \\
&= E(x_m(t)x_m^*(t)x_i(t)x_j^*(t)) - E(x_m(t)x_m^*(t))E(x_i(t)x_j^*(t)) - E(x_m(t)x_i(t))E(x_m^*(t)x_j^*(t)) \\
&\quad - E(x_m(t)x_j^*(t))E(x_m^*(t)x_i(t)) \\
&= \mathrm{Cum}\{x_m(t), x_m^*(t), x_i(t), x_j^*(t)\} = \mathbf{C}_m(i,j).
\end{aligned} \tag{34}$$

And hence $E(\Delta\mathbf{C}_m) = E(\widehat{\mathbf{C}}_m) - \mathbf{C}_m = \mathbf{O}$. Analogously, we may easily verify that $E(\Delta\mathbf{D}_m) = E(\widehat{\mathbf{D}}_m) - \mathbf{D}_m = \mathbf{O}$. It then follows that $E(\Delta\mathbf{U}) = \mathbf{O}$, and accordingly,

$$\begin{aligned}
E(\Delta\boldsymbol{\Xi}_{\mathrm{NP}}) &\simeq -\kappa\left(\kappa\mathbf{I} + \mathbf{R}_x^{\mathrm{H}}\mathbf{R}_x + \lambda\sum_{m=1}^{4}\mathbf{C}_m^{\mathrm{H}}\mathbf{C}_m\right)^{-1}\check{\mathbf{\Pi}} \\
&= -\kappa(\kappa\mathbf{I} + \mathbf{G})^{-1}\check{\mathbf{\Pi}} = \tilde{\mathbf{\Pi}},
\end{aligned} \tag{35}$$

which implies that the norm-penalized conjugate MI-ESPRIT matrix estimator is biased. In fact, from (26) we know that the norm-penalized MI-ESPRIT behaves as a uniform diagonal loader. The larger the κ, the more smoothed the solution, and the lower the variance of solution.

Additionally,

$$\begin{aligned}
||\tilde{\mathbf{\Pi}}||_F &= ||\left(\mathbf{I}_4 + \kappa^{-1}\mathbf{G}\right)^{-1}\check{\mathbf{\Pi}}||_F \\
&\leqslant ||\left(\mathbf{I}_4 + \kappa^{-1}\mathbf{G}\right)^{-1}||_F \cdot ||\check{\mathbf{\Pi}}||_F.
\end{aligned} \tag{36}$$

By definition, $\mathrm{rank}(\mathbf{G}) = Q$, and $\mathbf{G}$ is Hermitian and nonnegative-definite. Denote the Q positive eigenvalues of $\mathbf{G}$ as μ_q, then (note that $||\mathbf{X}||_F^2 = ||\mathbf{X}^{\mathrm{H}}||_F^2 = \mathrm{trace}(\mathbf{X}^{\mathrm{H}}\mathbf{X}) = \sum_j u_j(\mathbf{X}^{\mathrm{H}}\mathbf{X})$, where $u_j(\mathbf{X}^{\mathrm{H}}\mathbf{X})$ denotes the jth

eigenvalue of $\mathbf{X}^{\mathrm{H}}\mathbf{X}$)

$$||\tilde{\mathbf{\Pi}}||_F \left(\sqrt{4-Q+\sum_{q=1}^{Q}\left(\frac{1}{1+\kappa^{-1}\mu_q}\right)^2} \right) \cdot ||\mathbf{\Pi}||_F, \tag{37}$$

which implies that the bound of $||\tilde{\mathbf{\Pi}}||_F$ increases as κ increases. Moreover, $\left(\mathbf{I}+\kappa^{-1}\mathbf{G}\right)^{-1} = \mathbf{I}-\kappa^{-1}\mathbf{G}(\mathbf{I}+\kappa^{-1}\mathbf{G})^{-1}$, and then

$$\begin{aligned} ||(\mathbf{I}_4+\kappa^{-1}\mathbf{G})^{-1}||_F &= ||\mathbf{I}_4-\kappa^{-1}\mathbf{G}\left(\mathbf{I}_4+\kappa^{-1}\mathbf{G}\right)^{-1}||_F \\ &\leqslant ||\mathbf{I}_4||_F + ||\kappa^{-1}\mathbf{G}(\mathbf{I}_4+\kappa^{-1}\mathbf{G})^{-1}||_F \\ &\leqslant 2+||\kappa^{-1}\mathbf{G}||_F \cdot ||(\mathbf{I}_4+\kappa^{-1}\mathbf{G})^{-1}||_F. \end{aligned} \tag{38}$$

Thus, for a large κ such that $||\mathbf{G}||_F<\kappa$, i.e., $||\kappa^{-1}\mathbf{G}||_F<1$, we have $||(\mathbf{I}_4+\kappa^{-1}\mathbf{G})^{-1}||_F \leqslant \frac{2}{1-||\kappa^{-1}\mathbf{G}||_F}$, and hence,

$$||\tilde{\mathbf{\Pi}}||_F \leqslant \frac{2}{1-\kappa^{-1}||\mathbf{G}||_F} \cdot ||\mathbf{\Pi}||_F. \tag{39}$$

As $\kappa \to \infty$, $(1-\kappa^{-1}||\mathbf{G}||_F)^{-1} \to 1$, which indicates that $||\tilde{\mathbf{\Pi}}||_F$ is always bounded by $2||\mathbf{\Pi}||_F$. In fact, $||\tilde{\mathbf{\Pi}}||_F$ has a more strict upper-bound $||\mathbf{\Pi}||_F$ by noting that $\tilde{\mathbf{\Pi}}|_{\kappa\to\infty} = \breve{\mathbf{\Pi}}$.

4.2. Mean-squared-error (MSE) analysis

We here define the mean-squared-error (MSE) of ESPRIT matrix as follows:

$$\begin{aligned} \mathrm{MSE}(\Delta\mathbf{\Xi}_{NP}) \overset{\mathrm{def}}{=} E(||\Delta\mathbf{\Xi}_{NP}||_F^2) &= \sum_{m=1}^{4} E(\Delta^{\mathrm{H}}\mathbf{u}_m(\kappa\mathbf{I}+\mathbf{G})^{-2}\Delta\mathbf{u}_m) \\ &\quad + \sum_{m=1}^{4} \kappa^2 \mathbf{\psi}_m^{\mathrm{H}}(\kappa\mathbf{I}+\mathbf{G})^{-2}\mathbf{\psi}_m \end{aligned} \tag{40}$$

where $\Delta\mathbf{u}_m = \Delta\mathbf{U}(:,m)$, and $E(\Delta\mathbf{u}_m)=0$, $\mathbf{\psi}_m = \breve{\mathbf{\Pi}}(:,m)$. Express $\mathbf{G}$ in terms of its eigenvalues and eigenvectors. That is,

$$\mathbf{G} = \underbrace{[\mathbf{E}'_s, \mathbf{E}'_n]}_{\overset{\mathrm{def}}{=}\mathbf{E}'} \underbrace{\begin{bmatrix} \mathbf{\Sigma}'_s & \\ & \mathbf{O} \end{bmatrix}}_{\overset{\mathrm{def}}{=}\mathbf{\Sigma}'} \begin{bmatrix} \mathbf{E}'^{\mathrm{H}}_s \\ \mathbf{E}'^{\mathrm{H}}_n \end{bmatrix} = \mathbf{E}'\mathbf{\Sigma}'\mathbf{E}'^{\mathrm{H}}, \tag{41}$$

where $\mathbf{\Sigma}'_s = \mathrm{diag}(\mu_1,\ldots,\mu_Q)$, and $\{\mu_m>0, m=1,2,\ldots,Q\}$. Then, $(\kappa\mathbf{I}+\mathbf{G})^{-2} = \mathbf{E}'(\mathbf{\Sigma}'+\kappa\mathbf{I})^{-2}\mathbf{E}'^{\mathrm{H}}$, and

$$\begin{aligned} &E(||\Delta\mathbf{\Xi}_{\mathrm{NP}}||_F^2) \\ &= \sum_{m=1}^{4}\left(\sum_{n=1}^{Q}\frac{\chi^2_{m,n}}{(\mu_n+\kappa)^2} + \sum_{n=Q+1}^{4}\frac{\chi^2_{m,n}}{\kappa^2}\right) + \kappa^2\sum_{m=1}^{4}\left(\sum_{n=1}^{Q}\frac{\chi'^2_{m,n}}{(\mu_n+\kappa)^2}\right) + \sum_{m=1}^{4}\left(\sum_{n=Q+1}^{4}\chi'^2_{m,n}\right) \end{aligned} \tag{42}$$

where $\chi^2_{m,n} = E(\mathbf{\Delta}^{\mathrm{H}}\mathbf{u}_m\mathbf{e}_n\mathbf{e}_n^{\mathrm{H}}\mathbf{\Delta}\mathbf{u}_m)$,, $\chi'^2_{m,n} = \mathbf{\psi}_m^{\mathrm{H}}\mathbf{e}_n\mathbf{e}_n^{\mathrm{H}}\mathbf{\psi}_m$, and $\mathbf{e}_n = \mathbf{E}'(:,n)$. For any $\kappa>0$ and a fixed λ, the first term (associated with the variance) in (42) is a monotonically decreasing function of κ, whereas the second term (associated with bias) is a monotonically increasing function of κ. The MSE of the norm-penalized CMI-ESPRIT generally trades off between the variance and bias and achieves the minimal value at some appropriate κ.

5. Perturbation analysis of the subspace-constraint ESPRIT matrix

5.1. Bias analysis

Denote

$$\Delta\boldsymbol{\Xi}_{\mathrm{SC}} = \widehat{\boldsymbol{\Xi}}_{\mathrm{SC}} - \breve{\boldsymbol{\Pi}}.$$

Since $\widehat{\boldsymbol{\Xi}}_{\mathrm{SC}} = (\widehat{\mathbf{H}}_1^{\mathrm{H}}\widehat{\mathbf{H}}_1)^{-1}\widehat{\mathbf{H}}_1^{\mathrm{H}}\widehat{\mathbf{F}}_2$, where $\widehat{\mathbf{H}}_1 \overset{\mathrm{def}}{=} [\sqrt{\kappa}\widehat{\mathbf{P}}_n, \widehat{\mathbf{R}}_x^{\mathrm{H}}, \sqrt{\lambda}\widehat{\mathbf{C}}_1^{\mathrm{H}}, \ldots, \sqrt{\lambda}\widehat{\mathbf{C}}_4^{\mathrm{H}}]^{\mathrm{H}}$, $\kappa \neq 0$, we have (using, in turn, $\Delta\boldsymbol{\Xi}_{\mathrm{SC}} = (\widehat{\mathbf{H}}_1^{\mathrm{H}}\widehat{\mathbf{H}}_1)^{-1}\widehat{\mathbf{H}}_1^{\mathrm{H}}\widehat{\mathbf{F}}_2 - \breve{\boldsymbol{\Pi}} = (\widehat{\mathbf{H}}_1^{\mathrm{H}}\widehat{\mathbf{H}}_1)^{-1}\widehat{\mathbf{H}}_1^{\mathrm{H}}(\widehat{\mathbf{F}}_2 - \widehat{\mathbf{H}}_1^{\mathrm{H}}\breve{\boldsymbol{\Pi}})$, and $\mathbf{F}_2 = \mathbf{H}_1\breve{\boldsymbol{\Pi}}$)

$$\begin{aligned}
\Delta\boldsymbol{\Xi}_{\mathrm{SC}} &= (\widehat{\mathbf{H}}_1^{\mathrm{H}}\widehat{\mathbf{H}}_1)^{-1}\widehat{\mathbf{H}}_1^{\mathrm{H}}(\Delta\mathbf{F}_2 - \Delta\mathbf{H}_1\breve{\boldsymbol{\Pi}}) \\
&\simeq (\mathbf{H}_1^{\mathrm{H}}\mathbf{H}_1)^{-1}\mathbf{H}_1^{\mathrm{H}}(\Delta\mathbf{F}_2 - \Delta\mathbf{H}_1\breve{\boldsymbol{\Pi}}) \\
&= -\left(\kappa\mathbf{P}_n + \mathbf{R}_x^{\mathrm{H}}\mathbf{R}_x + \lambda\sum_{m=1}^{4}\mathbf{C}_m^{\mathrm{H}}\mathbf{C}_m\right)^{-1} \\
&\quad \times \left(\mathbf{R}_x^{\mathrm{H}}(\Delta\mathbf{R}_x\breve{\boldsymbol{\Pi}} - \Delta\mathbf{R}_{x^*}) + \lambda\sum_{m=1}^{4}\mathbf{C}_m^{\mathrm{H}}(\Delta\mathbf{C}_m\breve{\boldsymbol{\Pi}} - \Delta\mathbf{D}_m) + \kappa\mathbf{P}_n\Delta\mathbf{P}_n\breve{\boldsymbol{\Pi}}\right) \\
&= -(\kappa\mathbf{P}_n + \mathbf{G})^{-1}(\Delta\mathbf{U} + \kappa\mathbf{P}_n\Delta\mathbf{P}_n\breve{\boldsymbol{\Pi}}),
\end{aligned} \tag{43}$$

where $\mathbf{H}_1 \overset{\mathrm{def}}{=} [\sqrt{\kappa}\mathbf{P}_n, \mathbf{R}_x^{\mathrm{H}}, \sqrt{\lambda}\mathbf{C}_1^{\mathrm{H}}, \ldots, \sqrt{\lambda}\mathbf{C}_4^{\mathrm{H}}]^{\mathrm{H}}$, $\Delta\mathbf{P}_n = \widehat{\mathbf{P}}_n - \mathbf{P}_n$. Let $\mathbf{w}_g$ be the eigenvector of $\mathbf{R}_x$ associated with eigenvalue w_g, where $g = 1, 2, 3, 4$. Then, from [23], we have

$$\begin{aligned}
\Delta\mathbf{w}_g &= \widehat{\mathbf{w}}_g - \mathbf{w}_g \\
&\simeq \sum_{h\neq g, h=1}^{4} \mathbf{w}_h \underbrace{\sum_{l_1=1}^{4}\sum_{l_2=1}^{4}\left(\frac{\mathbf{w}_h^*(l_1)[\widehat{\mathbf{R}}_x(l_1,l_2) - \mathbf{R}_x(l_1,l_2)]\mathbf{w}_g(l_2)}{w_g - w_h}\right)}_{\overset{\mathrm{def}}{=} F_{g,h}} \\
&= \sum_{h\neq g, h=1}^{4} F_{g,h}\mathbf{w}_h.
\end{aligned} \tag{44}$$

Moreover,

$$\begin{aligned}
\widehat{\mathbf{P}}_n &= \sum_{l=Q+1}^{4}\widehat{\mathbf{w}}_l\widehat{\mathbf{w}}_l^{\mathrm{H}} = \mathbf{I} - \sum_{l=1}^{Q}\widehat{\mathbf{w}}_l\widehat{\mathbf{w}}_l^{\mathrm{H}} \\
&= \mathbf{I} - \sum_{l=1}^{Q}(\mathbf{w}_l + \Delta\mathbf{w}_l)(\mathbf{w}_l + \Delta\mathbf{w}_l)^{\mathrm{H}}.
\end{aligned} \tag{45}$$

And

$$\Delta\mathbf{P}_n = \widehat{\mathbf{P}}_n - \mathbf{P}_n = -\sum_{l=1}^{Q}(\mathbf{w}_l\Delta\mathbf{w}_l^{\mathrm{H}} + \Delta\mathbf{w}_l\mathbf{w}_l^{\mathrm{H}} + \Delta\mathbf{w}_l\Delta\mathbf{w}_l^{\mathrm{H}}). \tag{46}$$

Thus, $E(\Delta\mathbf{P}_n) = -\sum_{l=1}^{Q}E(\Delta\mathbf{w}_l\Delta\mathbf{w}_l^{\mathrm{H}})$, and hence (noting $\mathbf{P}_n\mathbf{w}_k = \mathbf{0}$ for $k = 1, \ldots, Q$, and $\mathbf{w}_k^{\mathrm{H}}\mathbf{A} = \mathbf{O}$ for $k = Q+1, \ldots, 4$)

$$\begin{aligned}
\mathbf{P}_n E(\Delta\mathbf{P}_n)\breve{\boldsymbol{\Pi}} &= E(\mathbf{P}_n\Delta\mathbf{P}_n\breve{\boldsymbol{\Pi}}) \\
&= E(\mathbf{P}_n\Delta\mathbf{P}_n(\mathbf{A}\boldsymbol{\Phi}^{-2}\mathbf{A}^{+})^{\mathrm{H}}) \\
&= E\left\{\mathbf{P}_n\left[\sum_{g=1}^{Q}\left(\left(\sum_{h_1\neq g, h_1=1}^{4}F_{g,h_1}\mathbf{w}_{h_1}\right)\left(\sum_{h_2\neq g, h_2=1}^{4}F_{g,h_2}\mathbf{w}_{h_2}\right)^{\mathrm{H}}\right)\right](\mathbf{A}\boldsymbol{\Phi}^{-2}\mathbf{A}^{+})^{\mathrm{H}}\right\} \\
&= \mathbf{O}.
\end{aligned} \tag{47}$$

Then

$$E(\Delta\boldsymbol{\Xi}_{\mathrm{SC}}) = -(\kappa\mathbf{P}_n + \mathbf{G})^{-1}[E(\Delta\mathbf{U}) + \kappa E(\mathbf{P}_n\Delta\mathbf{P}_n\check{\mathbf{\Pi}})] \simeq \mathbf{O}. \tag{48}$$

It is seen that the subspace-constraint conjugate MI-ESPRIT is asymptotically unbiased, potentially owing to the fact that $\mathbf{P}_n\check{\mathbf{\Pi}} = \mathbf{O}$.

5.2. Mean-squared-error analysis

From (43), we have,

$$E(||\Delta\boldsymbol{\Xi}_{SC}||_F^2) = \sum_{m=1}^{4} E(\Delta^{\mathrm{H}}\mathbf{u}_m(\kappa\mathbf{P}_n + \mathbf{G})^{-2}\Delta\mathbf{u}_m) + \kappa^2 E\sum_{m=1}^{4}\boldsymbol{\psi}_m^{\mathrm{H}}\Delta\mathbf{P}_n^{\mathrm{H}}\mathbf{P}_n(\kappa\mathbf{P}_n + \mathbf{G})^{-2}\mathbf{P}_n\Delta\mathbf{P}_n\boldsymbol{\psi}_m. \tag{49}$$

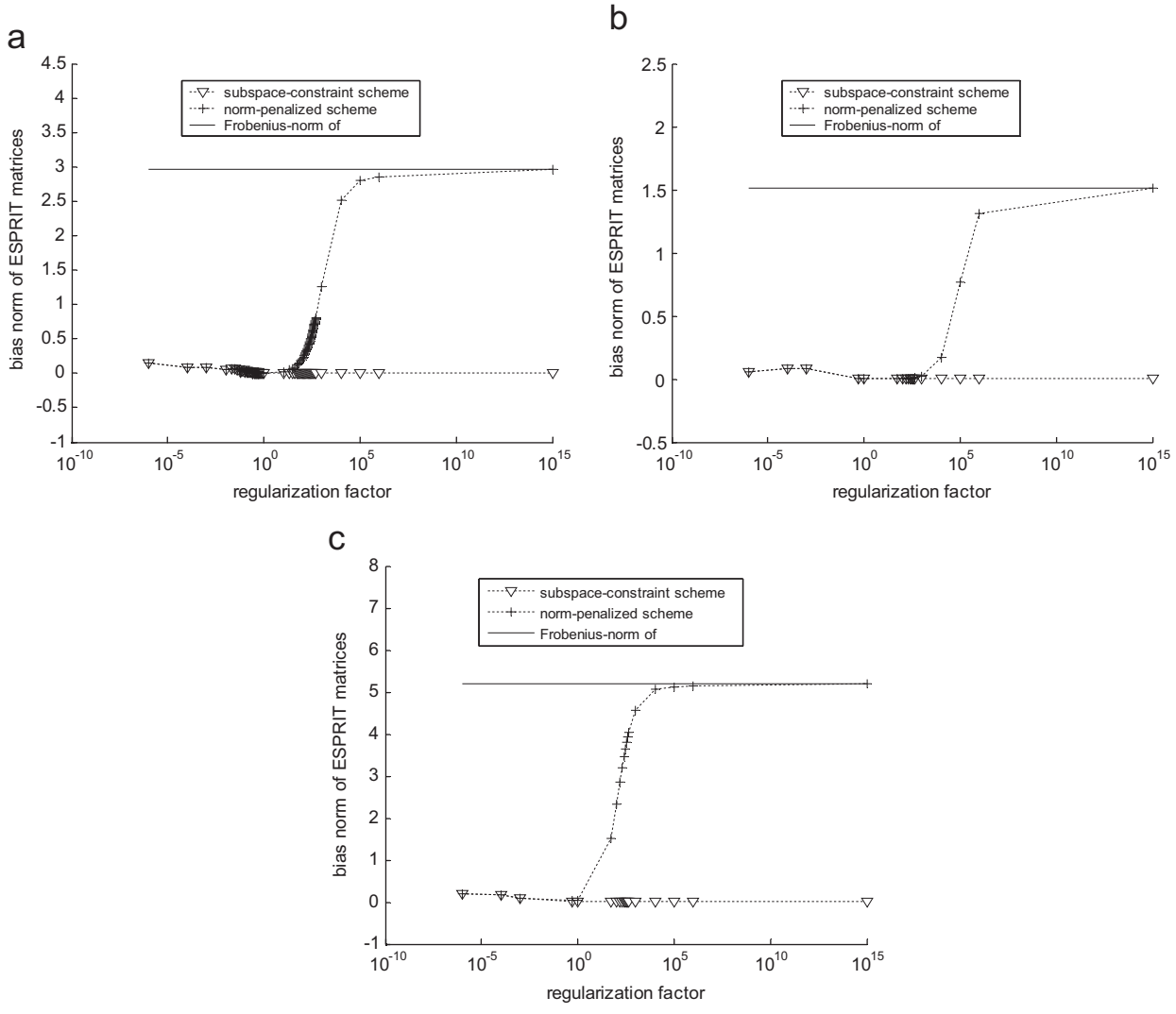

Fig. 2. Bias norm (i.e., $||\tilde{\mathbf{P}}||_{\mathrm{F}}$) of ESPRIT matrices. (a) the DOAs are (30°, 60°) and (45°, 90°); (b) the DOAs are (15°, 30°) and (60°, 120°); (c) the DOAs are (30°, 35°) and (45°, 50°).

Moreover, $\mathbf{P}_n = \mathbf{E}'_n(\mathbf{E}'_n)^{\mathrm{H}}$, and hence

$$\kappa\mathbf{P}_n + \mathbf{G} = [\mathbf{E}'_s, \mathbf{E}'_n] \underbrace{\begin{bmatrix} \boldsymbol{\Sigma}'_s & \\ & \kappa\mathbf{I} \end{bmatrix}}_{\stackrel{def}{=}\widetilde{\boldsymbol{\Sigma}}} \begin{bmatrix} \mathbf{E}'^{\mathrm{H}}_s \\ \mathbf{E}'^{\mathrm{H}}_n \end{bmatrix} = \mathbf{E}'\widetilde{\boldsymbol{\Sigma}}\,\mathbf{E}^H. \tag{50}$$

Then $(\kappa\mathbf{P}_n + \mathbf{G})^{-2} = \mathbf{E}'\tilde{\boldsymbol{\Sigma}}^{-2}\mathbf{E}'^{\mathrm{H}}$, and

$$E(||\Delta\boldsymbol{\Xi}_{\mathrm{SC}}||_F^2) = \sum_{m=1}^{4}\left(\sum_{n=1}^{Q}\frac{\chi^2_{m,n}}{\mu_n^2} + \sum_{n=Q+1}^{4}\frac{\tilde{\chi}^2_{m,n}}{\kappa^2}\right) + \sum_{m=1}^{4}\left(\sum_{n=Q+1}^{4}\tilde{\chi}^2_{m,n}\right), \tag{51}$$

where $\tilde{\chi}^2_{m,n} = \boldsymbol{\psi}_m^{\mathrm{H}}\Delta\mathbf{P}_n^{\mathrm{H}}\mathbf{e}_n\mathbf{e}_n^{\mathrm{H}}\Delta\mathbf{P}_n\boldsymbol{\psi}_m$. As a consequence, for any $\kappa > 0$ and a fixed λ, the MSE expression of the subspace constraint CMI-ESPRIT shown in (51) is nearly independent of κ. This is quite different from that of the norm-penalized CMI-ESPRIT discussed in Section 4.2. In addition, as $\kappa \to \infty$, those very smaller eigenvalues of $\widehat{\mathbf{R}}_x$, $\widehat{\mathbf{C}}_m$ are implicitly discarded (also known as eigenvalue truncation).

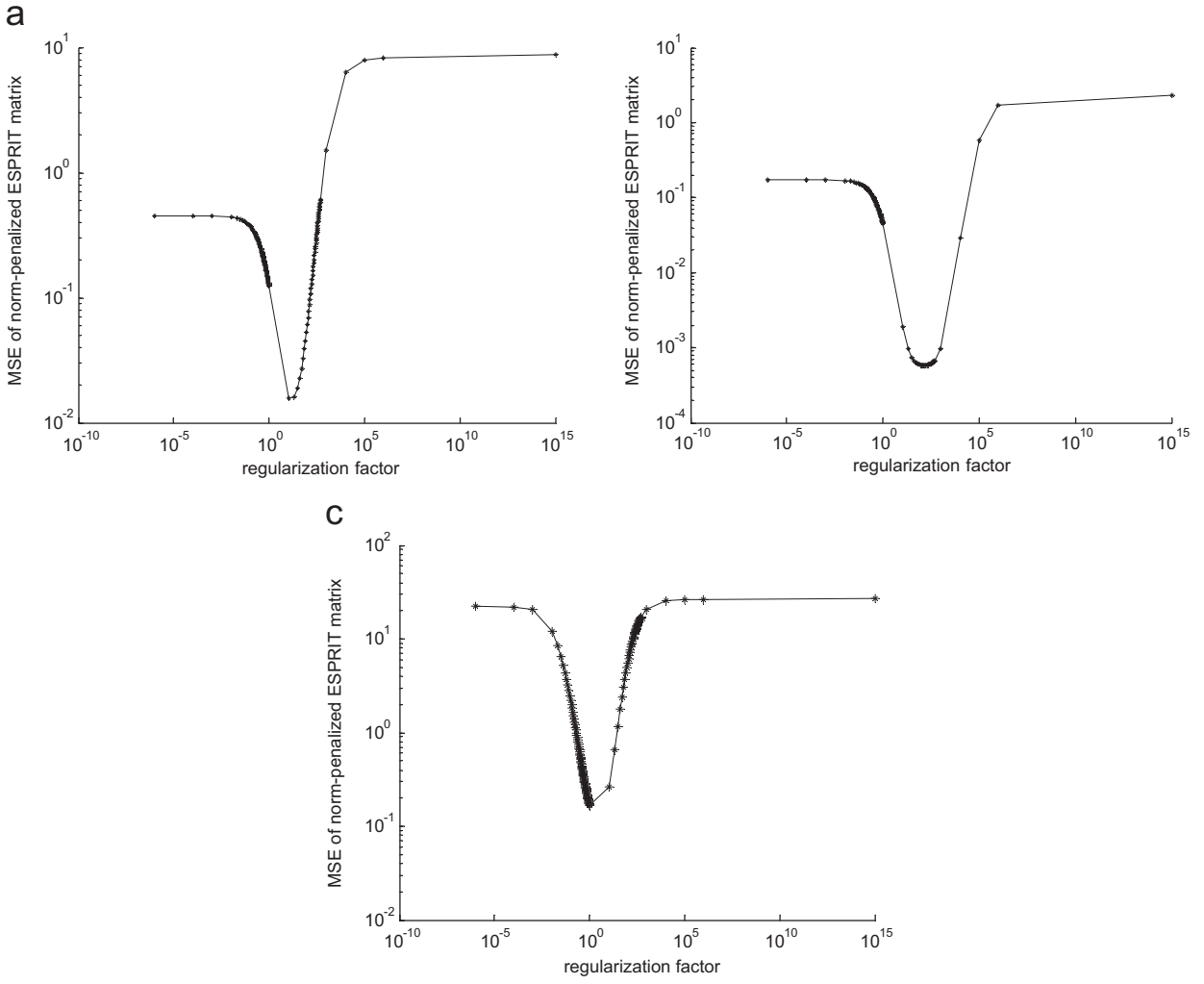

Fig. 3. MSE curves for norm-penalized ESPRIT matrix. (a) the DOAs are (30°, 60°) and (45°, 90°); (b) the DOAs are (15°, 30°) and (60°, 120°); (c) the DOAs are (30°, 35°) and (45°, 50°).

6. Numerical examples

We consider two independent BPSK signals from (30°, 60°) and (45°, 90°), respectively. The initial phases of the two signals are $\pi/7$ and $\pi/3$, respectively. The number of snapshot is 200. The signal to noise ratio (SNR) is 20 dB. In the simulation, only two cumulant matrix slices $\widehat{\mathbf{C}}_1$ and $\widehat{\mathbf{D}}_1$ are used. The regularization factors are varied over 10^{-6} and 10^{15}, and $\lambda = 10^{-4}$. The statistics shown are computed by 1000 independent trials. The bias norm of the two types of ESPRIT matrices are plotted in Fig. 2(a). For comparison, the possible upper-bound of the bias norm, i.e., $||\mathbf{\Pi}||_F$, is also included in the same figure. It is seen that the norm-penalized ESPRIT matrix estimator is biased and approaches the upper-bound as κ goes to infinite, whereas the subspace-constraint ESPRIT matrix estimator is unbiased. The MSE curves for the two methods are plotted in Figs. 3(a) and 4(a), respectively. The corresponding results for two signals from (15°, 30°), (60°, 120°) instead are provided in Figs. 2(b), 3(b) and 4(b). It is seen from Fig. 3 that there exists a unique optimal κ to make the MSE of norm-penalized ESPRIT matrix minimum. On the other hand, the curve shown in Fig. 4 indicates that the MSE of subspace-constraint ESPRIT matrix decreases all the time as κ increases. We finally consider two signals that have very close DOAs, that is, (30°, 35°), (45°, 50°). The corresponding results are

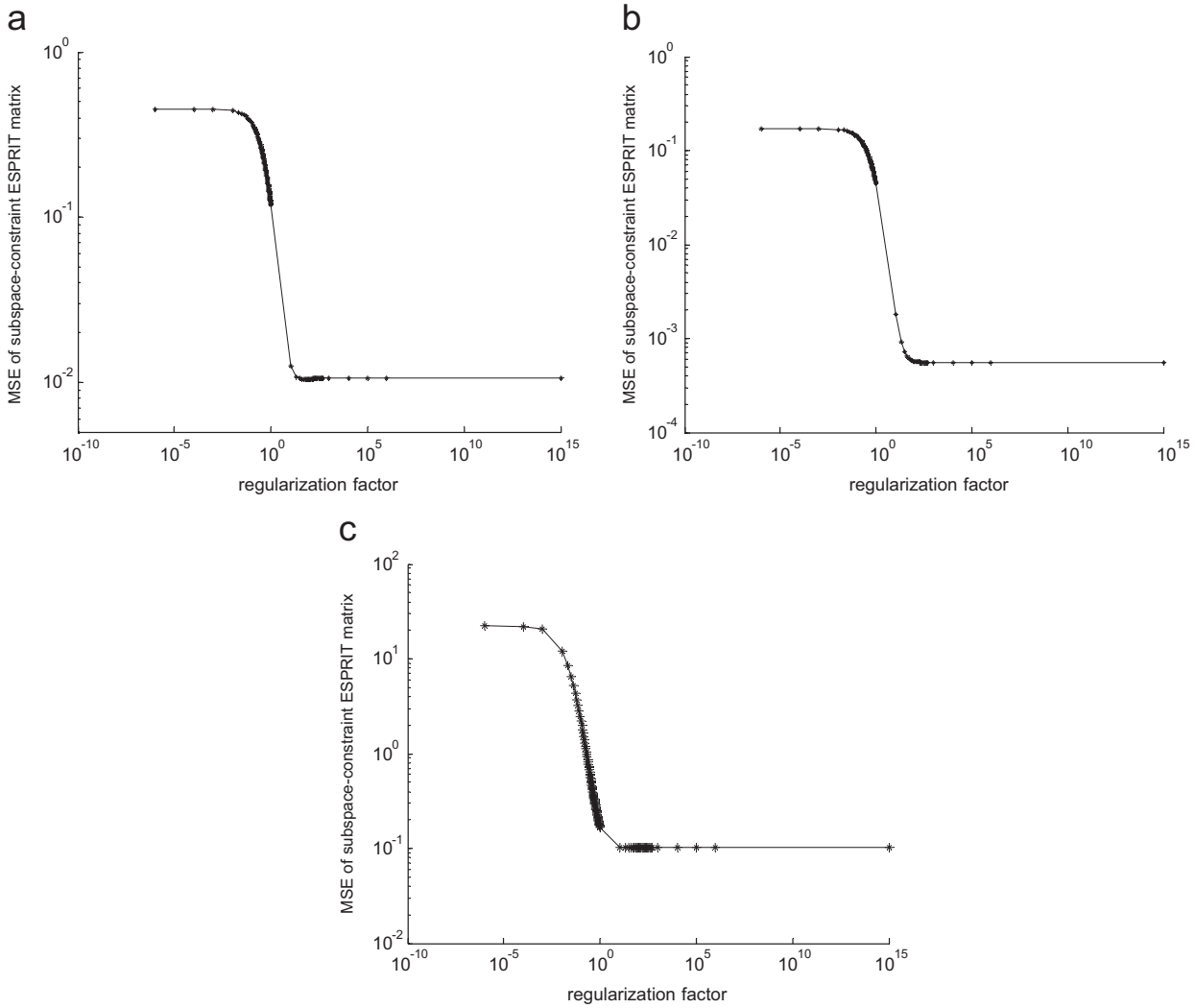

Fig. 4. MSE curve for subspace-constraint ESPRIT matrix. (a) The DOAs are (30°, 60°) and (45°, 90°); (b) the DOAs are (15°, 30°) and (60°, 120°); (c) the DOAs are (30°, 35°) and (45°, 50°).

presented in Figs. 2(c), 3(c) and 4(c), and similar trends are observed. These provided results have well validated the correctness of the discussions made earlier. Furthermore, from these showings we may find that, under a certain threshold (the closer DOAs appears to lead to the lower threshold), the bias terms of both methods maintain a very small (nearly of zero) and constant level. Hence, in these regions as the regularization parameters increase, the reduction of variances of both methods results in an MSE decrease (the variance decreases as regularization parameter increases to yield a more smoothing on the desired solution). However, in the regions above that threshold, there is a clear behavior difference between the two methods. For the subspace-constraint scheme, the bias term continues to be near zero and hence the MSE as well as variance reduces as the regularization parameter increases. For the norm-penalized scheme, however, the bias term increases rapidly and then quickly dominates the overall MSE term as the regularization parameter increases. As a consequence, the MSE term changes to be increased as regularization parameter increases. In addition, the attainable smallest MSE of the subspace-constraint scheme appears to be lower than that of norm-penalized scheme. Thus, the subspace-constraint scheme may be more attractive than the norm-penalized one with respect to optimum selection of regularization parameter as well as available performance potential.

7. Conclusions

In this paper, we have provided the first-order approximation-based perturbation analyses on two types of ESPRIT matrices in the CMI-ESPRIT algorithm involving norm-penalization and subspace-constraining, respectively. It has been shown that norm penalization can effectively smooth the solution but introduce bias at the same time. The subspace constraint scheme, on the other hand, smooth the solution without inducing bias. The CMI-ESPRIT algorithm and the analyses provided in this paper may be straightforwardly extended to single-vector-sensor-based linearly-polarized signal (noncircular) direction-finding for electromagnetic applications. To conclude the paper, we remark that examining the effect of the whitening factor λ used in the methods is also of great practical importance. The first author of this paper is presently investigating the optimum determination of the whitening factor λ with Gauss–Markov-based technique [25].

References

[1] A. Nehorai, E. Paldi, Acoustic vector-sensor array processing, IEEE Trans. Signal Process. 42 (1994) 2481–2491.
[2] C.B. Leslie, J.M. Kendall, J.L. Jones, Hydrophone for measuring particle velocity, J. Acoust. Soc. Am. 28 (1956) 711–715.
[3] G.L. D'Spain, W.S. Hodgkiss, G.L. Edmonds, The simultaneous measurement of infrasonic acoustic particle velocity and acoustic pressure in the ocean by freely drifting swallow floats, IEEE J. Oceanic Eng. 16 (1991) 195–207.
[4] P. Tichavský, K.T. Wong, M.D. Zoltowski, Near-field/far field azimuth and elevation angle estimation using a single vector hydrophone, IEEE Trans. Signal Process. 49 (2001) 2498–2510.
[5] M. Hawkes, A. Nehorai, Acoustic vector-sensor beamforming and Capon direction estimation, IEEE Trans. Signal Process. 46 (1998) 2291–2304.
[6] K.T. Wong, Blind beamforming/geolocation for wideband-FFHs with unknown hop-sequences, IEEE Trans. Aerospace Electron. Syst. 37 (2001) 65–75.
[7] K.T. Wong, M.D. Zoltowski, Closed-form underwater acoustic direction-finding with arbitrarily spaced vector hydrophones at unknown locations, IEEE J. Oceanic Eng. 22 (1997) 649–658.
[8] K.T. Wong, M.D. Zoltowski, Extended-aperture underwater acoustic multisource azimuth/elevation direction-finding using uniformly but sparsely spaced vector hydrophones, IEEE J. Oceanic Eng. 22 (1997) 659–672.
[9] K.T. Wong, M.D. Zoltowski, Self-initiating MUSIC-based direction finding in underwater acoustic particle velocity-field beamspace, IEEE J. Oceanic Eng. 25 (2000) 262–273.
[10] P. Chargé, Y. Wang, J. Saillard, A non-circular sources direction finding method using polynomial rooting, Signal Processing 81 (2001) 1765–1770.
[11] M. Haardt, F. Römer, Enhancements of unitary ESPRIT for non-circular sources, in: Proceedings of the ICASSP, 2004, pp. 101–104.
[12] J. Galy, C. Adnet, Blind separation of non-circular sources, in: Proceedings of the Tenth IEEE Workshop on Statistical Signal and Array Processing, 2000, pp. 315–318.
[13] J.P. Delmas, Stochastic Cramér–Rao bound for noncircular signals with application to DOA estimation, IEEE Trans. Signal Process. 52 (2004) 3192–3199.
[14] H. Abeida, J.P. Delmas, Gaussian Cramer–Rao bound for direction estimation of non-circular signals in unknown noise fields, IEEE Trans. Signal Process. 53 (2005) 4610–4618.
[15] R. Roy, T. Kailath, ESPRIT—estimation of signal parameters via rotational invariance techniques, IEEE Trans. Acoustics Speech Signal Process. 37 (1989) 984–995.

[16] Y.-G. Xu, Z.-W. Liu, On single-vector-sensor direction finding for linearly polarized sources having non-circular constellations, in: Proceedings of the Eighth International Conference on Signal Processing, Guilin, China, 2006.
[17] E. Gónen, J.M. Mendel, Applications of cumulants to array processing—Part III: blind beamforming for coherent signals, IEEE Trans. Signal Process. 45 (1997) 2252–2264.
[18] A. Ferreol, P. Chevalier, On the behavior of current second and higher order blind source separation methods for cyclostationary sources, IEEE Trans. Signal Process. 48 (2000) 1712–1725.
[19] A.L. Swindlehurst, B. Ottersten, R. Roy, T. Kailath, Multiple invariant ESPRIT, IEEE Trans. Signal Process. 40 (1992) 867–881.
[20] M. Stojanovic, Recent advances in high-speed underwater acoustic communications, IEEE J. Oceanic Eng. 21 (1996) 125–136.
[21] E. Petit, G. Jourdain, An efficient self-recovering adaptive algorithm for BPSK signals transmitted through underwater acoustic channels, in: Proceedings of the ICASSP, 1995, pp. 3159–3162.
[22] D.B. Kilfoyle, A.B. Baggeroer, The state of the art in underwater acoustic telemetry, IEEE J. Oceanic Eng. 25 (2000) 4–27.
[23] N. Yuen, B. Friedlander, Asymptotic performance analysis of ESPRIT, higher order ESPRIT, and virtual ESPRIT algorithms, IEEE Trans. Signal Process. 44 (1996) 2537–2550.
[24] P. Stoica, T. Söderström, V. Symonite, On estimating the noise power in array processing, Signal Processing 26 (1992) 205–220.
[25] A. Eriksson, P. Stoica, T. Söderström, Markov-based eigenanalysis method for frequency estimation, IEEE Trans. Signal Process. 42 (1994) 586–594.